AIP Applied Physics Letters

On-chip electron-impact ion source using carbon nanotube field emitters

Christopher A. Bower, Kristin H. Gilchrist, Jeffrey R. Piascik, Brian R. Stoner, Srividya Natarajan, Charles B. Parker, Scott D. Wolter, and Jeffrey T. Glass

Citation: Applied Physics Letters **90**, 124102 (2007); doi: 10.1063/1.2715457
View online: http://dx.doi.org/10.1063/1.2715457
View Table of Contents: http://scitation.aip.org/content/aip/journal/apl/90/12?ver=pdfcov
Published by the AIP Publishing

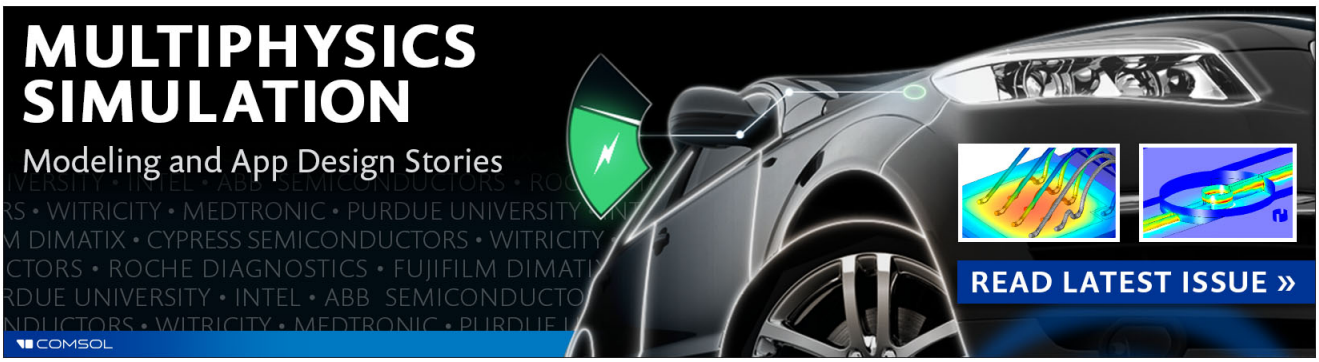

On-chip electron-impact ion source using carbon nanotube field emitters

Christopher A. Bower, Kristin H. Gilchrist,[a] Jeffrey R. Piascik, and Brian R. Stoner
Center for Materials and Electronic Technologies, RTI International, North Carolina 27709

Srividya Natarajan, Charles B. Parker, Scott D. Wolter, and Jeffrey T. Glass
Department of Electrical and Computer Engineering, Duke University, North Carolina 27708

(Received 10 January 2007; accepted 20 February 2007; published online 20 March 2007)

A lateral on-chip electron-impact ion source utilizing a carbon nanotube field emission electron source was fabricated and characterized. The device consists of a cathode with aligned carbon nanotubes, a control grid, and an ion collector electrode. The electron-impact ionization of He, Ar, and Xe was studied as a function of field emission current and pressure. The ion current was linear with respect to gas pressure from 10^{-4} to 10^{-1} Torr. The device can operate as a vacuum ion gauge with a sensitivity of approximately 1 Torr^{-1}. Ion currents in excess of 1 μA were generated.
 [DOI: 10.1063/1.2715457]

The generation of gas phase ions by electron impact is a common technique in the fields of mass spectrometry[1] and vacuum science.[2] In mass spectrometry, electron-impact sources ionize gas phase analytes prior to mass separation and ion detection. In vacuum science, ion vacuum gauges, residual gas analyzers, and He leak detectors all operate using electron-impact ionization. Thermionic cathodes are reliable and effective for many applications; however, the power consumption associated with heating these cathodes is a major limitation in developing miniature field-portable ion sources. In many emerging applications such as field-portable mass spectrometers,[3] the power required to heat the thermionic electron source could exceed the combined power requirements of all other system components. Therefore field emission cold cathodes which nominally operate at room temperature are attractive for some electron-impact applications. Kornienko *et al.*[4] evaluated a cold cathode electron-impact ion source made from an array of diamond-coated silicon whiskers for application in an ion trap mass spectrometer. Others have reported traditional vacuum ion gauges utilizing carbon nanotubes[5,6] (CNTs) and molybdenum tips[7] as the electron source. Chalamala *et al.*[8] reported on the real-time pressure measurement inside field emission displays using integrated field emitters for electron-impact ionization. Additional benefits of field emission sources are the fast turn on and the ability to run in a pulsed mode. Thermionic technology does not readily scale down to microdevices, while field emission devices are naturally microscale and have the potential to generate larger emitted current densities. Due to their robust mechanical structure and chemical stability, it is believed that CNT field emitters may be well suited for these applications despite reports that they are susceptible to ion impact damage.[9]

This letter describes the fabrication and characterization of an on-chip electron-impact ion source for potential application as an integrated cold cathode vacuum gauge or as a small, power efficient, ion source for mass spectrometry applications. Figure 1(a) depicts how a similar device was previously characterized as a vacuum triode with both the grid and the anode biased positively with respect to the grounded cathode.[10,11] Figure 1(b) illustrates how electron-impact ionization can be studied using the same device. The positively biased grid controls the field emission of electrons from the cathode. Some percentage of the emitted electrons pass through the grid apertures into the region between the grid and the negatively biased ion collector. The electrons are decelerated by the collector bias and ultimately deflected back towards the grid if the collector voltage is large enough. If an electron-impact ionization event occurs in this region between the grid and the collector, the positively charged ion will be accelerated towards the collector electrode. If an electron-impact event occurs in the region between the cathode and grid, the generated ion will be accelerated into the cathode, possibly damaging the electron emitters.

Electron-impact ionization theory has established the following relationship for the generated ion current (I_i):[2] $I_i = kI_e l\rho\sigma(E)$, where k is a device specific geometrical constant, I_e is the electron current, l is the electron path length, ρ is the neutral gas density, and $\sigma(E)$ is the ionization cross section which depends on gas type and electron energy (E). Electron-impact ionization cross sections for most atoms and molecules[12] indicate that gases display broad maxima of impact ionization probability with electrons of energy between 70 and 100 eV. A field emitted electron has some initial energy and then rapidly accelerates in the electric field between the grid and the cathode. Some of the emitted electron current passes through the grid apertures into the ionization volume between the positively biased grid and the negatively biased collector. The collector bias will influence the total path length (l) of the electron. For a grid voltage of 250 V, the electrons will have energies of approximately 250 eV as they pass through the grid aperture into the ionization volume. The electrons will be decelerated by the negatively biased ion collector and at two segments along the electron

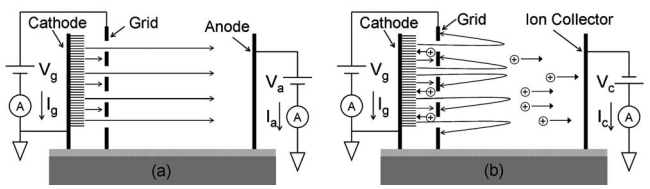

FIG. 1. Schematic illustration of the different configurations for operating the device as a (a) triode or (b) ion source.

[a]Electronic mail: kgilchrist@rti.org

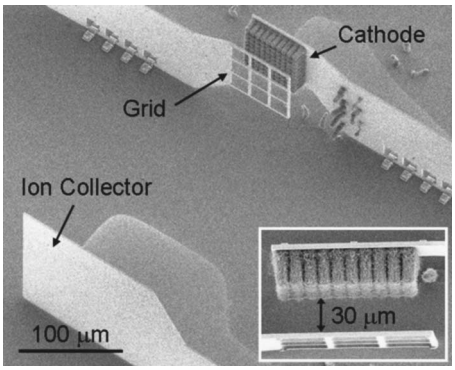

FIG. 2. Scanning electron micrograph of the electron-impact ion source with inset showing top-down view of the CNT cathode and grid.

path length (l) they will fall within the 70–100 eV energy range for maximum ionization probability. Ions generated in the ionization region will be accelerated to the ion collector and be measured as ion current (I_i).

The device was fabricated using a well-known polycrystalline silicon microelectromechanical system (MEMS) process that has been described in detail.[13] As discussed in previous studies,[10,11] the nonstoichiometric silicon nitride layer provided by the MEMS foundry does not yield adequate electrical insulation for vacuum electronic applications. Thus, the devices described here were fabricated on modified substrates with a 10 μm thermal silicon dioxide layer. Scanning electron microscope micrographs of a representative device are shown in Fig. 2. The details of the device assembly and cathode fabrication have been previously reported.[10,11] Briefly, the polycrystalline silicon structures that form the device electrodes were initially parallel with the substrate surface and embedded in highly doped silicon dioxide. After the MEMS fabrication, the sacrificial silicon dioxide was etched in hydrofluoric acid to release the electrode panels. The catalyst for CNT growth, in this case 50 Å of iron, was selectively evaporated onto the cathode using an integrated shadow mask. The CNTs were grown using microwave plasma chemical vapor deposition[14,15] with ammonia/methane gas chemistry. Electron microscopy revealed multiwalled CNTs with an average diameter of approximately 30 nm. The CNT length was controlled by varying the growth time. After CNT deposition, the panels were manually rotated and locked in place normal to the substrate using a tongue-in-groove MEMS technique. The device was mounted and wire bonded to a ceramic board for testing. The specific device characterized here has a cathode-to-grid spacing of 50 μm before CNT deposition, a cathode-to-grid spacing of 30 μm after CNT deposition, and a grid-to-collector spacing of 280 μm. The cathode is a 70×70 μm^2 panel and the grid is a 3×3 array of 20×20 μm^2 apertures, with a 2.5 μm grid wire.

The characterization of the electron-impact ion source was carried out at room temperature in a vacuum chamber with a base pressure of 1×10^{-6} Torr. A gas manifold with an adjustable leak valve (Granville Phillips 203) was used to control the chamber atmosphere and pressure. The chamber pressure was measured using a cold cathode ion gauge below 10^{-4} Torr and a calibrated capacitance manometer above 10^{-4} Torr. Unlike the ion gauge, the capacitance manometer does not exhibit strong gas dependence. A semiconductor

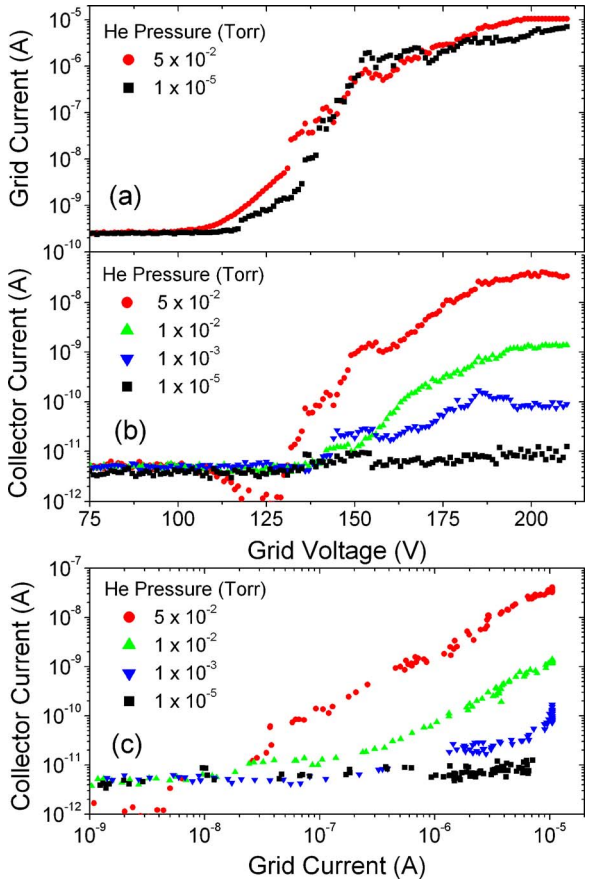

FIG. 3. (Color online) (a) Grid current (I_g) vs grid voltage (V_g), (b) collector current (I_c) vs grid voltage, and (c) collector current vs measured grid current. The legend indicates the He chamber pressure for each data set. The ion collector voltage (V_c) was held at −210 V during these measurements.

characterization system (Keithley 4200-SCS) was used for supplying voltages and measuring currents.

The electron field emission properties of the integrated CNT cathodes were characterized prior to ionization experiments. During ionization experiments, field emission data were obtained by recording both the cathode and grid currents. Figure 3(a) is a plot of the measured grid current (I_g) versus grid voltage (V_g) with the ion collector voltage (V_c) biased to −210 V so that the field emitted electrons from the cathode were captured by the grid. The electric fields required to generate 1 nA and 1 μA of electron current were 5 and 6 V/μm, respectively. These devices were routinely capable of generating field emitted electron current in excess of 50 μA. Characterizing the device as an electron triode, where some percentage of electrons pass through the grid apertures to the positively biased anode, allows for the determination of the ratio of anode current to grid current (I_a/I_g). This ratio varies across devices but typically ranged from 2 to 4. During ionization experiments, a quantitative measure of the electron current (I_e) that passes into the ionization volume is unavailable because all of the emitted electrons are eventually captured by the grid, as shown in Fig. 1(b). However, the measured grid current (I_g) should be proportional to the electron current (I_e) during electron-impact ionization ($I_g \alpha I_e$). In a He atmosphere, the emitted electron current did not exhibit a strong dependence on gas pressure. Figure 3(a) shows the emitted electron current (I_g) measured at both 10^{-5} Torr and 50 mTorr. Figure 3(b) shows the measured

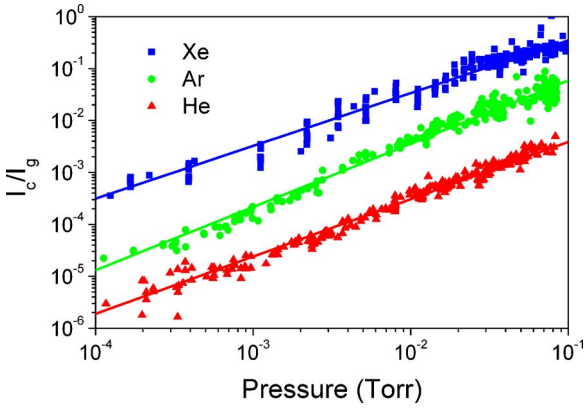

FIG. 4. (Color online) Ion collector current normalized by the electron grid current (I_c/I_g) vs the measured chamber pressure for helium, argon, and xenon.

collector current (I_c), in this case He ions, versus applied grid voltage. The ion current increases as He chamber pressure increases, as expected from electron-impact theory. At the chamber base pressure the measured ion collector current is less than 10 pA, while at a pressure of 50 mTorr the ion current approaches 100 nA, representing four orders of magnitude change. The ion current begins to saturate as the grid voltage is increased, which corresponds to the saturation in the emitted electron current shown in Fig. 3(a). Figure 3(c) is a plot of the collector current (I_c) versus grid current (I_g), which follows a linear relationship as expected from the electron-impact model. Linear fits were performed on the data in the higher grid current regime ($I_g > 1$ μA) and the measured slopes correspond to the number of ions created per electron. For He, the values are 1.2×10^{-4} at 10 mTorr and 3.8×10^{-3} at 50 mTorr, which are comparable to the familiar 1000 to 1 rule associated with electron-impact efficiencies.[1]

Figure 4 shows the measured normalized ion current (I_c/I_g) versus pressure for three inert gases (He, Ar, Xe). The grid voltage (V_g) was set to establish 1 μA of measured grid current (I_g), and the collector voltage (V_c) was biased to −210 V. The grid and collector currents were recorded along with the pressure (P) from the capacitance manometer while gas was slowly introduced into the chamber with the leak valve. The ion current recorded at the collector increased linearly with gas pressure, as expected from electron-impact theory. The qualitative trends across gases in Fig. 4 follow expectations based on the high ionization probability of Xe and the low ionization probability of He. With I_g set to 10 μA, the device was capable of generating Xe ion currents in excess of 2.5 μA at 0.1 Torr, corresponding to an ion current density of approximately 50 mA/cm^2.

This linear dependence of normalized ion current on gas pressure shown in Fig. 4 indicates that the device can be used as a pressure gauge. Vacuum ion gauges typically operate in the range where the ratio of ion current to electron current (I_i/I_e) is linear with respect to gas pressure. The sensitivity factor (S) of an ion gauge is defined by the relation $I_i/I_e = SP$, where P is the gas pressure.[2] Typical ion gauges can have sensitivity factors in excess of 1000 because long electron paths allow for many ionization events. Schulz and Phelps designed an ion gauge that could be used at pressures up to 1 Torr by decreasing the electron path length to approximately 2500 μm to minimize scattering and maximize the collector efficiency.[16] In our device, the electron path length is a function of the collector bias but is expected to be less than 600 μm. Therefore, as observed in Fig. 4, the gauge can operate at relatively high pressures. The slopes of the data in Fig. 4 correspond to the gauge sensitivity (1.1 Torr^{-1} for He, 1.2 Torr^{-1} for Ar, and 1.0 Torr^{-1} for Xe). For these short electron path lengths that enable higher pressure operation, a small sensitivity compared to more traditional ion gauges is expected.

Initial lifetime studies of the CNT cathode under electron-impact conditions were performed in a 1 mTorr He environment. There was no noticeable degradation in the electron or ion currents after 1 h of continuous operation. Future testing will include additional gases and longer time periods. It is expected that reactive gases will have a negative impact on the performance of the cathode.[17] However, it may be possible to operate the devices using a pulsed mode where ions generated between the cathode and grid are swept to the collector rather than bombard the electron emitters.

In summary, an on-chip electron-impact ion source built using MEMS fabrication techniques and utilizing a CNT field emission electron source was achieved. Ionization data for He, Ar, and Xe as a function of the electron emission current and chamber pressure were presented. Operation as a miniature vacuum ion gauge at higher pressures than traditional ion gauges was demonstrated. If such ion sources can be proven robust, they will be useful in numerous applications requiring small size and low power consumption compared to thermionic ion sources.

This work was supported by NSF (Contract No. ECS-0428540) and NASA (Contract No. NNL-04-AA21A).

[1] E. de Hoffman and V. Stroobant, *Mass Spectrometry Principles and Applications* (Wiley, London, 2002), pp. 11–13.
[2] J. F. O'Hanlon, *A User's Guide to Vacuum Technology* (Wiley, New York, 1989), pp. 89–94, and 123.
[3] E. R. Badman and G. R. Cooks, J. Mass Spectrom. **35**, 659 (2000).
[4] O. Kornienko, P. T. A. Reilly, W. B. Whitten, and J. M. Ramsey, Anal. Chem. **72**, 559 (2000).
[5] C. Dong and G. R. Myneni, Appl. Phys. Lett. **84**, 5443 (2004).
[6] I.-M. Choi and S.-Y. Woo, Appl. Phys. Lett. **87**, 173104 (2005).
[7] C. Dong and G. R. Myneni, J. Vac. Sci. Technol. A **17**, 2026 (1999).
[8] B. R. Chalamala, R. H. Reuss, and K. A. Dean, Appl. Phys. Lett. **79**, 2648 (2001).
[9] K. A. Dean and B. R. Chalamala, Appl. Phys. Lett. **75**, 3017 (1999).
[10] C. Bower, W. Zhu, D. Shalom, D. Lopez, L. H. Chen, P. L. Gammel, and S. Jin, Appl. Phys. Lett. **80**, 3820 (2002).
[11] C. Bower, D. Shalom, W. Zhu, D. Lopez, G. P. Kochanski, P. L. Gammel, and S. Jin, IEEE Trans. Electron Devices **49**, 1478 (2002).
[12] L. J. Kieffer and G. H. Dunn, Rev. Mod. Phys. **38**, 1 (1966).
[13] J. Carter, A. Cowen, B. Hardy, R. Mahadevan, M. Stonefield, and S. Wilcenski, The PolyMUMPS Design Handbook, MEMSCAP Inc., Durham, NC, 2005 (available at http://www.memscap.com/mumps/documents/PolyMUMPs.DR.v11.pdf).
[14] H. Cui, O. Zhou, and B. R. Stoner, J. Appl. Phys. **88**, 6072 (2000).
[15] C. Bower, O. Zhou, W. Zhu, D. J. Werder, and S. Jin, Appl. Phys. Lett. **77**, 2767 (2000).
[16] G. J. Schulz and A. V. Phelps, Rev. Sci. Instrum. **28**, 1051 (1957).
[17] J.-M. Bonard, H. Kind, T. Stockli, and L.-O. Nilsson, Solid-State Electron. **45**, 893 (2001).